J Pharmacol Sci **125**, 274 – 282 (2014)

Journal of Pharmacological Sciences

Full Paper

Overexpression of PEP-19 Suppresses Angiotensin II–Induced Cardiomyocyte Hypertrophy

Yang-yang Xie[1], Meng-meng Sun[1], Xue-fang Lou[2], Chen Zhang[3], Feng Han[3], Bo-ya Zhang[4], Ping Wang[1,*a], and Ying-mei Lu[2,*b]

[1]*College of Pharmaceutical Sciences, Zhejiang University of Technology, Hangzhou 310014, China*
[2]*School of Medicine, Zhejiang University City College, Hangzhou 310058, China*
[3]*College of Pharmaceutical Sciences, Zhejiang University, Hangzhou 310058, China*
[4]*School of Medicine, Ningbo University, Ninbo 315000, China*

Received October 18, 2013; Accepted May 1, 2014

Abstract. The precise molecular mechanisms leading to disturbance of Ca^{2+}/calmodulin-dependent intracellular signalling in cardiac hypertrophy remains unclear. As an endogenous calmodulin regulator protein, the pathophysiology role of PEP-19 during cardiac hypertrophy was investigated in the present study. We here demonstrated that PEP-19 protein levels are significantly elevated in the aortic banding model in vivo and angiotensin II–induced cardiomyocyte hypertrophy in vitro. Consistent with inhibitory actions of PEP-19 on cardiomyocyte hypertrophy, induction of CaMKII and calcineurin activation as well as hypertrophy-related genes including atrial natriuretic peptide (ANP) and brain natriuretic peptide (BNP) was significantly inhibited by PEP-19 transfection. Moreover, PEP-19 partially ameliorates angiotensin II–induced elevation of phospho-phospholamban (Thr-17) and sarcoplasmic reticulum Ca^{2+} release in cardiomyocytes. Together, our results suggest that PEP-19 attenuates angiotensin II–induced cardiomyocyte hypertrophy via suppressing the disturbance of CaMKII and calcineurin signaling.

Keywords: angiotensin II, calmodulin kinase II, calcineurin, PEP-19, cardiomyocyte hypertrophy

Introduction

A number of cellular and molecular mechanisms are involved in the development of cardiac hypertrophy (1). The alternation in the intracellular Ca^{2+} concentration is a primary stimulus for the cardiohypertrophic response (2, 3). Calmodulin is a widespread transducer of intracellular Ca^{2+} signaling, which is considered to be influenced by Ca^{2+} ions. The Ca^{2+}-activated calmodulin has major signalling targets involved in the stimulation of hypertrophic gene transcription of the delta isoform of Ca^{2+}/Calmodulin-dependent protein kinase II (CaMKIIδ) and the Ca^{2+}/Calmodulin-activated serine/threonine phosphatase, calcineurin (CaN) (4, 5). The CaN-mediated hypertrophic response may lead to the heart failure (6 – 8). Pathological cardiac hypertrophy have been related to G-protein–coupled receptors, e.g., β1 receptors for epinephrine and norepinephrine, AT1 receptor for angiotensin II, and ET receptor for endothelin 1 (9, 10).

PEP-19, a 7.6-kDa polypeptide containing 61 amino acids, is selectively expressed in neurons (11 – 13), and PEP-19 mRNA expression distributes in human peripheral organs such as kidney, prostate, uterus, and heart (14). PEP-19 plays a role in regulation of calmodulin, as do similar members of the IQ motif family of proteins such as neuromodulin (GAP-43), neurogranin (RC3), and CAP-19 (15, 16). Moreover, PEP-19 has been shown to inhibit apoptotic processes in PC12 cells and elicit a neuroprotective effect in neurodegenerative disorders (17 – 19). It is proposed that PEP-19 has neuroprotective properties, which might be mediated through calmodulin inhibition following excitotoxic insults by glutamate (20). However, its role during the pathological process of cardiac hypertrophy remains elusive.

In the present study, we firstly report that PEP-19 is

Corresponding authors.
*[a]wangping45@zjut.edu.cn, *[b]luym@zucc.edu.cn
Published online in J-STAGE
doi: 10.1254/jphs.13208FP

induced both in aortic banding-induced cardiac hypertrophy in vivo and angiotensin II–induced cardiomyocyte hypertrophy in vitro. The key finding of our study are that PEP-19 overexpression depresses angiotensin II–induced cardiomyocyte hypertrophy, along with decreased disturbance of CaMKII and CaN activation.

Materials and Methods

Experimental surgical procedure

Male Sprague-Dawley rats weighing 180 – 200 g (8 – 9 weeks of age) were subjected to the abdominal aortic banding procedure for induction of cardiac hypertrophy as described previously (21). Rats were anesthetized, the abdominal aorta was exposed under sterile conditions through a midline abdominal incision, and a blunted 25-gauge needle (outside diameter, 0.5 mm) was placed between the right and left renal arteries. A ligature (6-0 silk) was snugly tied around both the renal artery and the needle. The needle was then removed, leaving the internal diameter of the aorta approximately equal to that of the needle. Sham-operated animals had an untied ligature placed in the same location. After surgery, animals were housed under controlled environmental conditions with food and water ad libitum.

Primary cardiomyocytes culture and transfection

The cardiomyocyte cultures were isolated by enzymatic disassociation of 1 – 3-day-old neonatal rat hearts has been detailed previously (3). In brief, cardiomyocytes were cultured in 35-mm dishes overnight in DMEM media supplemented with 10% fetal bovine serum, penicillin/streptomyocin (100 units/ml). The cells were transfected using 4 μl lipofectamine TM 2000 reagent (Invitrogen) and empty vector (pcDNA3.1) or active pcDNA3.1-PEP-19 vector. After transfection for 12 h, new serum-free DMEM was added to cells and supplemented with angiotensin II (100 nM) for another 48-h culture.

Immunocytochemistry

After transfection and angiotensin II stimulation, the cardiomyocytes were fixed in 4% formaldehyde for cell size measurement using immunocytochemistry as previously described (3). In brief, cells were incubated for 3 h at room temperature with rhodamine-conjugated Phalloidin (1:300; Molecular Probes, Eugene, OR, USA) in PBS containing 1% BSA. Cell images were taken by an Olympus fluorescence microscope, and the cell surface area of the cells was measured quantitatively using NIH Image program 1.63 software. All cells from randomly selected fields in 3 independent culture plates were examined for each condition (at least 100 myocytes per group). The cell surface area in control cells was expressed as 100%.

Western blot analysis

Cultured cells were washed with cold PBS and stored at −80°C until immunoblotting analysis was performed (3). Tissue samples were homogenized in 500 μL homogenizing buffer containing 50 mM Tris–HCl (pH 7.4), 0.5% Triton X-100, 4 mM EGTA, 10 mM EDTA, 1 mM Na_3VO_4, 30 mM sodium pyrophosphate, 50 mM NaF, 100 nM calyculin A, 50 μg/mL leupeptin, 25 μg/mL pepstatin A, 50 μg/mL trypsin inhibitor, and 1 mM dithiothreitol (DTT). Insoluble material was removed by a 20-min centrifugation at 15,000 × *g*. After determining protein concentration in fractions using Bradford's solution, samples containing equivalent amounts of protein were applied to 15% acrylamide denaturing gels (SDS-PAGE) (22). Equal amounts of proteins were separated on 10% – 15% SDS-PAGE gels and then transferred to an Immobilon PVDF transfer membrane for 2 h at 70 V. Membranes were blocked in 30 mM Tris-HCl (pH 7.4), 150 mM NaCl and 0.1% Tween 20 (TBS-T) containing 5% fat-free milk powder for 1 h at room temperature and incubated with anti-PEP-19 (1:1000) or antibodies against CaMKII and phospho-CaMKIIδ (rabbit polyclonal antibodies, 1:2000 dilution), calcineurin (rabbit polyclonal antibody, 1:2000), phospho-phospholamban (PLB, Thr-17; rabbit polyclonal antibody, 1:1000), phosphor-NFATc3 (Ser 265, rabbit polyclonal antibody; 1:200), or β-actin (mouse monoclonal antibody; 1:10,000) overnight at 4°C (23 – 25). After washing, membranes were incubated 60 min at room temperature with the appropriate horseradish peroxidase (HRP)-conjugated secondary antibody diluted in TBS-T. Immunoreactive proteins were visualized using the enhanced chemiluminescence detection system (Amersham Life Science, Buckinghamshire, UK).

Quantitative real-time RT–PCR

A quantitative analysis of atrial natriuretic peptide (ANP) and brain natriuretic peptide (BNP) mRNA expression in cultured cardiomyocytes was investigated by real-time polymerase chain reaction. Total RNA was extracted from cardiomyocytes by Trizol Reagent (Life Technologies, Inc., Carlsbad, CA, USA). Two micrograms of total RNA was reverse-transcribed using a Reverse Transcription System (Promega, Madison, WI, USA) according to manufacturer's protocol. PCR amplification was performed using a CFX 96 Real-Time PCR Detection System (Bio-Rad, Hercules, CA, USA). All reactions were performed in triplicate. The following oligonucleotide primers were used: For ANP: 5′-TGG GCTCCTTCTCCATCACC-3′ and 5′-GCCAAAAGGC

CAGGAAGAGG-3′; BNP: 5′-CTTGGGCTGTGAC GGGCTGAG-3′ and 5′-GCTGGGGAAAGAAGAGCC GCA-3′; and β-actin: 5′-CGTCCACCCGCGAGTAC AAC-3′ and 5′-TCCTTCTGACCCATACCCAC-3′. All transcripts were normalized to those of β-actin.

Sarcoplasmic reticulum Ca^{2+} measurement using Fura-2

Sarcoplasmic reticulum calcium concentration was detected by using Fura-2 (3). In brief, neonatal ventricular myocytes were cultured on glass coverslips and maintained in the growth medium. Briefly, after transfection with empty vector (pcDNA3.1) or active pcDNA3.1-PEP-19 vector for 12 h and then treated with fresh DMEM supplement with angiotensin II (100 M) for another 48 h culture, myocytes were loaded with the Ca^{2+}-sensitive dye Fura-2 acetoxymethyl ester (2.5 μM) for 30 min before measurement of Ca^{2+} levels in a chamber on the stage of an inverted microscope. When Ca^{2+} fluorescence levels came to steady state (2 min), 10 mM caffeine was applied for 10 s by a picosptitzer. The amplitude of caffeine-induced Ca^{2+} transient was used as an index of sarcoplasmic reticulum Ca^{2+} content. Changes in caffeine-induced Ca^{2+} release from the sarcoplasmic reticulum were determined using a ratio of the fluorescence emission at 510 nm in response to excitation at 340 and 380 nm.

Cellular electrophysiology

Current clamp recordings for cultured cardiomycoyte were performed by using the patch clamp technique (27). In brief, cardiomyocytes were visualized with an infrared-sensitive CCD camera with a × 40 water-immersion lens (Olympus). Action potentials were recorded with the use of a MultiClamp 700B amplifier Digidata 1440A analog-to-digital converter and pClamp 10.2 software (Axon Instruments/Molecular Devices, Sunnyvale, CA, USA). For current clamp recordings, patch pipettes (3 – 4 MΩ) filling solution consisted of 110 mM KCl, 5 mM Na_2ATP, 11 mM EGTA, 10 mM HEPES, 1 mM $CaCl_2$, 1 mM $MgCl_2$ (pH adjusted to 7.3 with KOH); and the bath solution consisted of 132 mM NaCl, 4.8 mM KCl, 10 mM HEPES, 1.2 mM $CaCl_2$, 2 mM $MgCl_2$ (pH adjusted to 7.3 with NaOH).

Statistical analyses

The data were analysed with *t*-tests when the means between 2 groups were compared. For multi-group comparisons, statistical significance was determined using one-way ANOVA followed by a post hoc Tukey's test. All data are expressed as the mean ± S.E.M. A value of $P < 0.05$ was considered to be significant.

Results

The cardiac hypertrophic response induced PEP-19 in vivo and in vitro

In the present study, subrenal banding of the abdominal aorta method was used to induce cardiac hypertrophy in the rats. Our results showed that after 4 weeks pressure overload treatment (PO 4W), the heart size was enlarged and the wall of ventricle also thickened (Fig. 1A). Here, we demonstrated that PEP-19 was undetectable in the neonatal and one month rat heart (Fig. 1B). However, the PEP-19 was detected at the 2nd and 4th week after abdominal aortic banding (PO 2W, 4W) (Fig. 1: B, C). It was reported that angiotensin II level markedly increased after 6 weeks of aortic banding surgery (28). Consistently, we also found the PEP-19 protein levels were induced after 24 h angiotensin II treatment in neonatal cardiomyocytes (Fig. 1D).

Effects of PEP-19 overexpression on angiotensin II–induced cardiomyocyte hypertrophy

We next investigate whether PEP-19 is a cause of cardiomyocyte hypertrophy or has an anti-hypertrophic function. Firstly, we examined morphological change of cardiomyocytes while transfected with empty vector or PEP-19 with or without angiotensin II treatment. Our results suggested that pcDNA3.1-PEP-19 transfection significantly attenuated angiotensin II–induced increase in surface area of cardiomyocytes (Fig. 2A), indicating it plays an inhibitory role on the cardiomyocyte hypertrophy. Moreover, ANP and BNP mRNA was significantly lower in cardiomyocytes expressing pcDNA3.1-PEP-19 vs. empty vector–transfected cardiomyocytes in the presence of angiotensin II (Fig. 2B).

PEP-19 inhibits angiotensin II–induced CaMKII and CaN activation

In order to elucidate the mechanism of PEP-19 on cardiomyocyte hypertrophy, we examined its effect on the autophosphorylation of CaMKII and CaN level. We observed a significant increase in phosphorylated CaMKII$\delta_{B/C}$ levels after exposure with angiotensin II occurred (Fig. 3). By contrast, our data demonstrated that PEP-19 transfection partially abolished the autophosphorylation of CaMKII$\delta_{B/C}$ in angiotensin II–treated cardiomyocytes (Fig. 3). In addition, CaN protein level was significantly elevated after angiotensin II stimulation, whereas it was inhibited after PEP-19 transfection (Fig. 4A). We then measured the phosphorylation level of NFATc3 (Ser-256) to further confirm whether hypertrophy was stimulated through the CaN pathway. Consistently, the results showed that phospho-NFATc3 (Ser-256) was decreased after PEP-19 transfection in

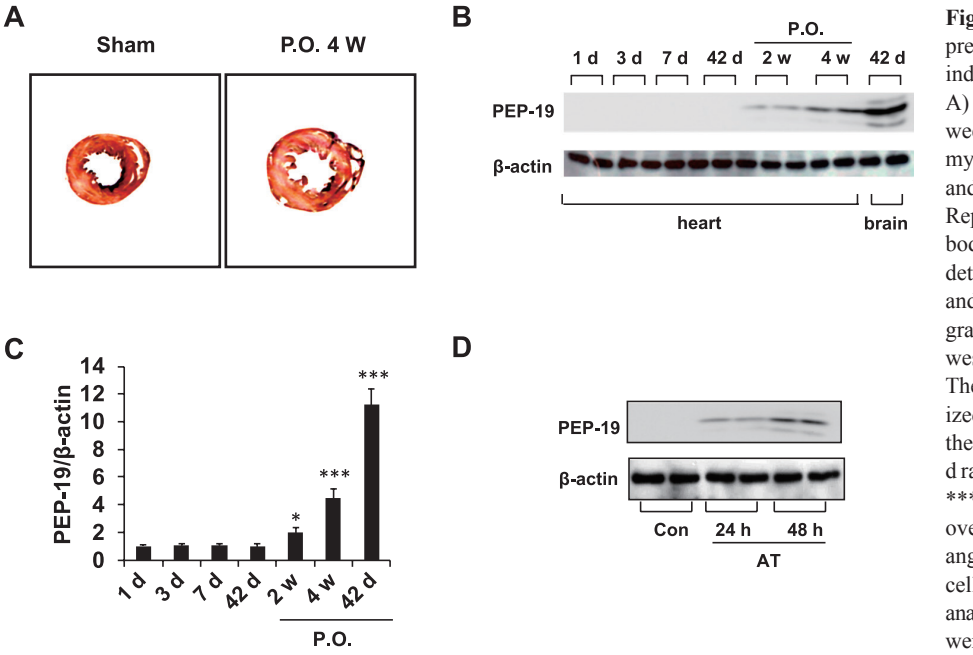

Fig. 1. In vivo induction of PEP-19 by pressure overload and angiotensin II–induced myocardial hypertrophy in vitro. A) After abdominal aortic banding for 4 weeks, Cross-sectional images of cardiomyocytes were stained with hematoxylin and eosin. P.O., pressure overload. B) Representative immunoblots with antibody specific for PEP-19: the peptide was detected in neonatal and adult rat heart and brain. P.O., pressure overload. C) Bar graphs show densitometric analysis of western blot of PEP-19 protein in (B). The protein level of PEP-19 was normalized to β-actin and expressed relative to the ratio in 1 d rats. The ratio obtained in 1 d rats was assigned a value of 1. $^{*}P < 0.05$, $^{***}P < 0.001$ vs. 1 d rats. P.O., pressure overload. D) After stimulation with angiotensin (AT) for 24 h and 48 h, the cells were collected for immunoblots analysis. Immounreactive bands of PEP-19 were detected as a 12 – 14 kDa doublet.

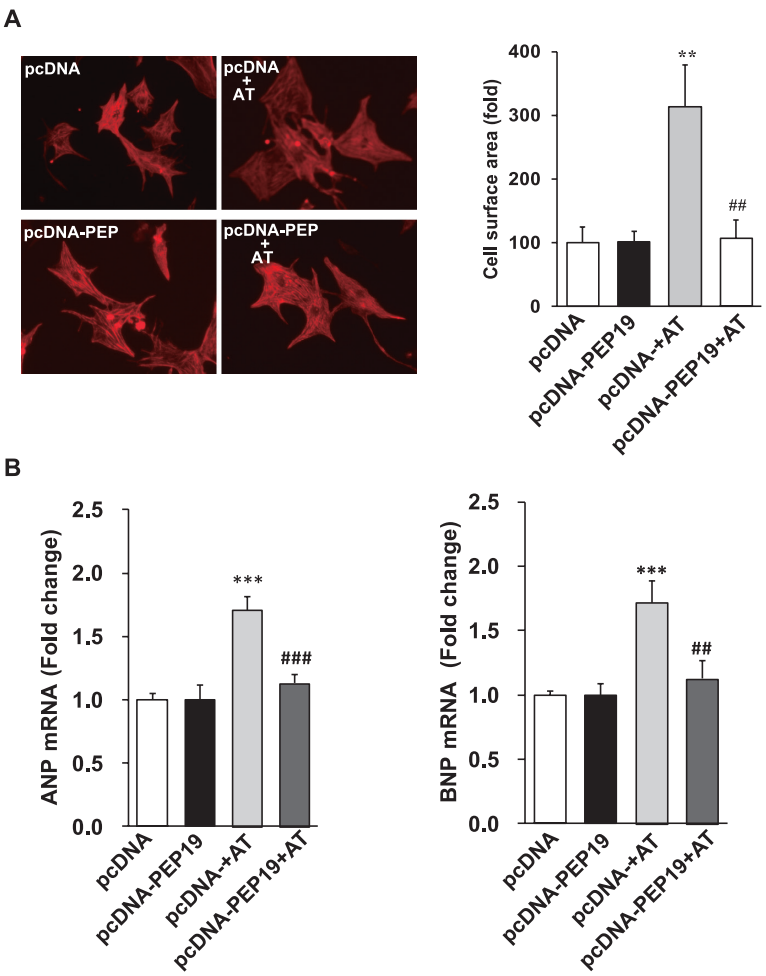

Fig. 2. Overexpression of PEP-19 inhibits angiotensin II–induced ANP and BNP mRNA expression. After transfection with empty vector (pcDNA3.1) or (pcDNA3.1-PEP-19) for 24 h, cardiomyocytes were incubated with or without angiotensin II (AT, 100 nM) for another 24 h. A) Cell size results are expressed as relative surface area standardized to the means surface areas of pcDNA in each experiment. $^{**}P < 0.01$ vs. pcDNA, $^{\#\#}P < 0.01$ vs. treatment with pcDNA + AT. pcDNA:pcDNA3.1. B) Quantification of ANP and BNP mRNA by real-time PCR. After transfection with empty vector (pcDNA3.1) or (pcDNA3.1-PEP-19) for 24 h, cardiomyocytes were incubated with or without angiotensin II (AT, 100 nM) for another 24 h. The mRNA level of ANP and BNP were normalized to β-actin and expressed relative to the ratio in vector-transfected control cells. $^{***}P < 0.001$ vs. pcDNA, $^{\#\#}P < 0.01$, $^{\#\#\#}P < 0.001$ vs. pcDNA + AT.

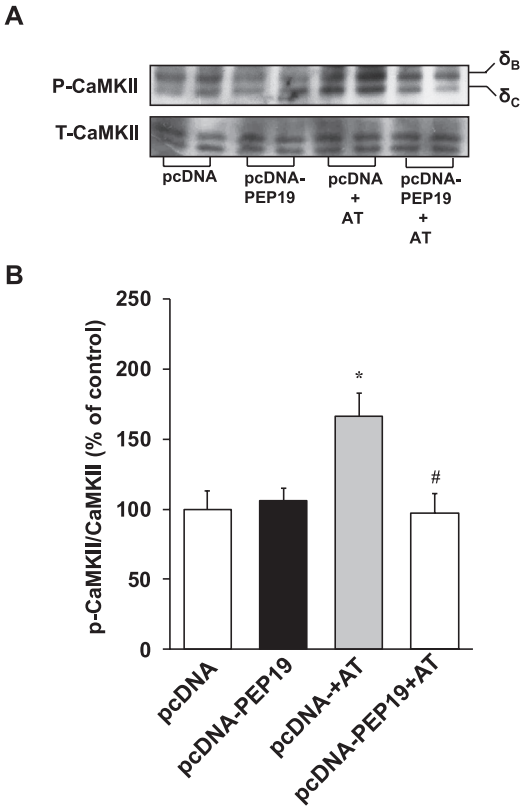

Fig. 3. Transfection of active PEP-19 inhibits angiotensin II–induced auto-phosphorylation of CaMKII. After transfection with empty vector (pcDNA3.1) or (pcDNA3.1-PEP-19) for 24 h, cardiomyocytes were incubated with or without angiotensin II (AT, 100 nM) for another 24 h. Extracts were prepared for blotting, and immunoblots performed with an anti-CaMKII antibody showed equal protein loading. Quantitative analysis of the 54/56 kDa autophosphorylated CaMKII$\delta_{B/C}$ band was performed by densitometry. Data are means ± S.E.M. of 3 independent experiments performed in triplicate. *$P < 0.05$ vs. pcDNA, $^{\#}P < 0.05$ vs. pcDNA + AT.

angiotensin II–treated cardiomyocytes (Fig. 4B).

Effect of PEP-19 on sarcoplasmic reticulum calcium signaling

Sarcoplasmic reticulum Ca^{2+} signaling has been established as being involved in the hypertrophic effects of angiotensin II as well as in the induction of cardiac hypertrophy (3). Here, greater phosphorylation of PLB at Thr-17 was observed in hypertrophic cardiomyocytes at 48 h with agonist treatment (Fig. 5A). By contrast, the increased phosphorylation of PLB upon angiotensin II treatment was blocked by PEP-19 overexpression (Fig. 5A). Moreover, we measured the Ca^{2+} content of the sarcoplasmic reticulum by assessing caffeine-induced Ca^{2+} release in cultured cardiomyocytes at 48 h. The Fura-2 ratio at 340/380 nm was not significantly different among the 4 groups in terms of the baseline. When Ca^{2+} release from the sarcoplasmic reticulum was triggered by the application of 10 mM caffeine, the transient Ca^{2+} elevation at 48 h increased 1.5-fold by angiotensin II treatment compared to the control cells (Fig. 5B). By contrast, the integrative volumes of the Ca^{2+} transient was significantly reduced by PEP-19 in comparison to angiotensin II–treated cardiomyocytes (Fig. 5B).

Effect of PEP-19 on membrane action potential

To determine whether angiotensin II stimulation can alter the cellular electrophysiology of cardiomyocytes, we performed current clamp studies on ventricular cardiomyocytes. The measure of membrane capacitance (C_m) and cardiac membrane input resistance (R_{in}) in cardiomyocytes is an index of their excitability, usually referred to as passive electrical properties and derived referring to an equivalent circuit. In the present study, we found that action potential morphologies from angiotensin II–stimulated cells reveal decreased cell excitability (Fig. 6A), whereas there were significant differences in the resting membrane potential (angiotensin II–treated cells, −31.38 ± 8.47 mV, $P < 0.001$ vs. control, −53.17 ± 6.03 mV); in R_{in} (angiotensin II–treated cells, 245.16 ± 17.58 MΩ, $P < 0.01$ vs. control, 576.49 ± 54.96 MΩ); in C_m (angiotensin II–treated cells, 40.45 ± 4.49 pF, $P < 0.01$ vs. control, 20.60 ± 2.20 pF). However, PEP-19 transfection significantly affect angiotensin II–induced the changes in resting membrane potential (49.58 ± 1.48 mV, $P < 0.05$ vs. angiotensin II–treated cells), in R_{in} (388.46 ± 50.90 MΩ, $P < 0.05$ vs. angiotensin II–treated cells), and C_m (27.79 ± 2.92 pF, $P < 0.05$ vs. angiotensin II–treated cells) (Fig. 6B).

Discussion

PEP-19 is firstly regarded as a neuronal expressed polypeptide that acts as an endogenous negative regulator of calmodulin by inhibiting the association of calmodulin with enzymes and other proteins. The altered expression in PEP-19 is associated with neurodegenerative disease (15, 29). Until now, the role of PEP-19 during the pathological process of hypertrophy remains largely unknown. In the present study, we documented that PEP-19 was inducible and detectable in the heart of animals under pressure overload. Moreover, we suggest that PEP-19 elicits antihypertrophic action through inhibition of CaMKII and CaN activation during development of cardiomyocyte hypertrophy.

Cardiac hypertrophy leading to heart failure is associated with abnormal intracellular Ca^{2+} regulation and impaired myocardial contractility (3). Calmodulin activity is modulated by both free Ca^{2+} levels and its binding to

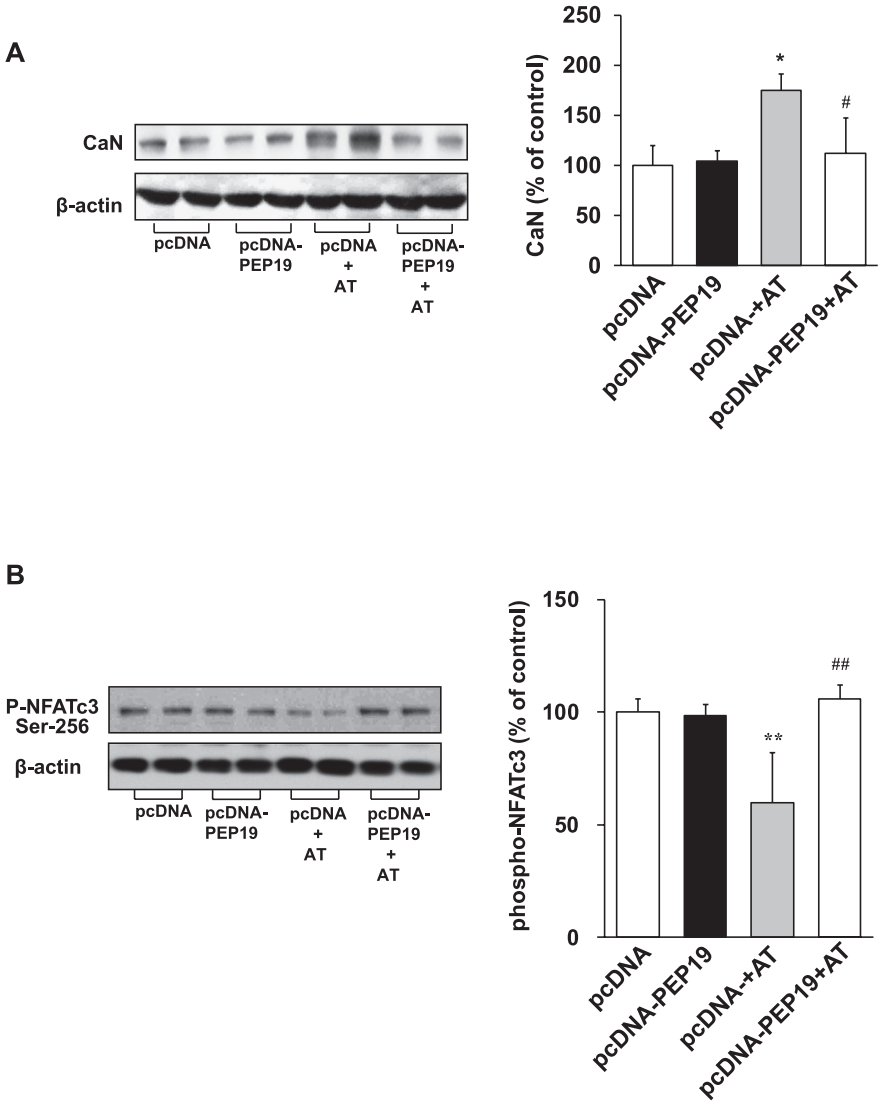

Fig. 4. Transfection of active PEP-19 inhibits angiotensin II–induced CaN protein overexpression and p-NFATc3 dephosphorylation. After transfection with pcDNA3.1-PEP-19 and stimulation with angiotensin II, extracts were prepared for immunoblot analysis. A) Representative image of an immunoblot performed by using anti-calcineurin antibody. Data are means ± S.E.M. of 3 independent experiments performed in triplicate. $^{*}P < 0.05$ vs. pcDNA, $^{\#}P < 0.05$ vs. pcDNA+AT. B) Representative image of an immunoblot performed by using anti-p-NFATc3 (ser-256) antibody. β-Actin was used as a loading control. Results are means ± S.E.M. of 3 independent experiments performed in triplicate. $^{**}P < 0.01$ vs. pcDNA, $^{\#\#}P < 0.01$ vs. pcDNA + AT.

IQ motif proteins (30 – 32). In the present study, we firstly found that pressure-overload induced the elevation of PEP-19 in the heart of rats, whereas the PEP-19 is undetectable in the control animals. PEP-19 was originally described in the central nervous system (11), but PEP-19 is also inducible in lactating breast and during osteogenic differentiation of bone marrow stem cells, which require high Ca^{2+} levels (33, 34).

To determine whether PEP-19 induced by hypertrophic stress participates in the pathological process of cardiac hypertrophy, PEP-19 was transfected into rat neonatal cardiomyocytes and its effect on cardiac hypertrophy and related cell signaling were addressed in the intact cardiomyocytes. Recently we reported that a novel antagonist of calmodulin inhibits the various calmodulin-dependent enzymes in a competitive manner and exerts a powerful cardioprotective action during the process of cardiac hypertrophy (35, 36). On the other hand, PEP-19 inhibited apoptosis in PC-12 cells and protected HEK293T cells against death due to Ca^{2+} overload (19, 20). Here, we found that PEP-19 transfection effectively reduced cardiac hypertrophy, as assessed by measuring the angiotensin II–induced changes in the cell surface of cardiomyocytes. Consistently, PEP-19 transfection also significantly reduced angiotensin II–induced elevation of ANP and BNP mRNA levels.

CaMKII and CaN are Ca^{2+}-CaM binding proteins that play important roles in the development of cardiac hypertrophy. The present study indicated that PEP-19 significantly decreased angiotensin II–induced autophosphorylation of CaMKII and activity of CaN. We previously reported that involvement of calmodulin in the regulation of cellular growth is of particular interest because the disturbance of Ca^{2+}/Calmodulin-dependent

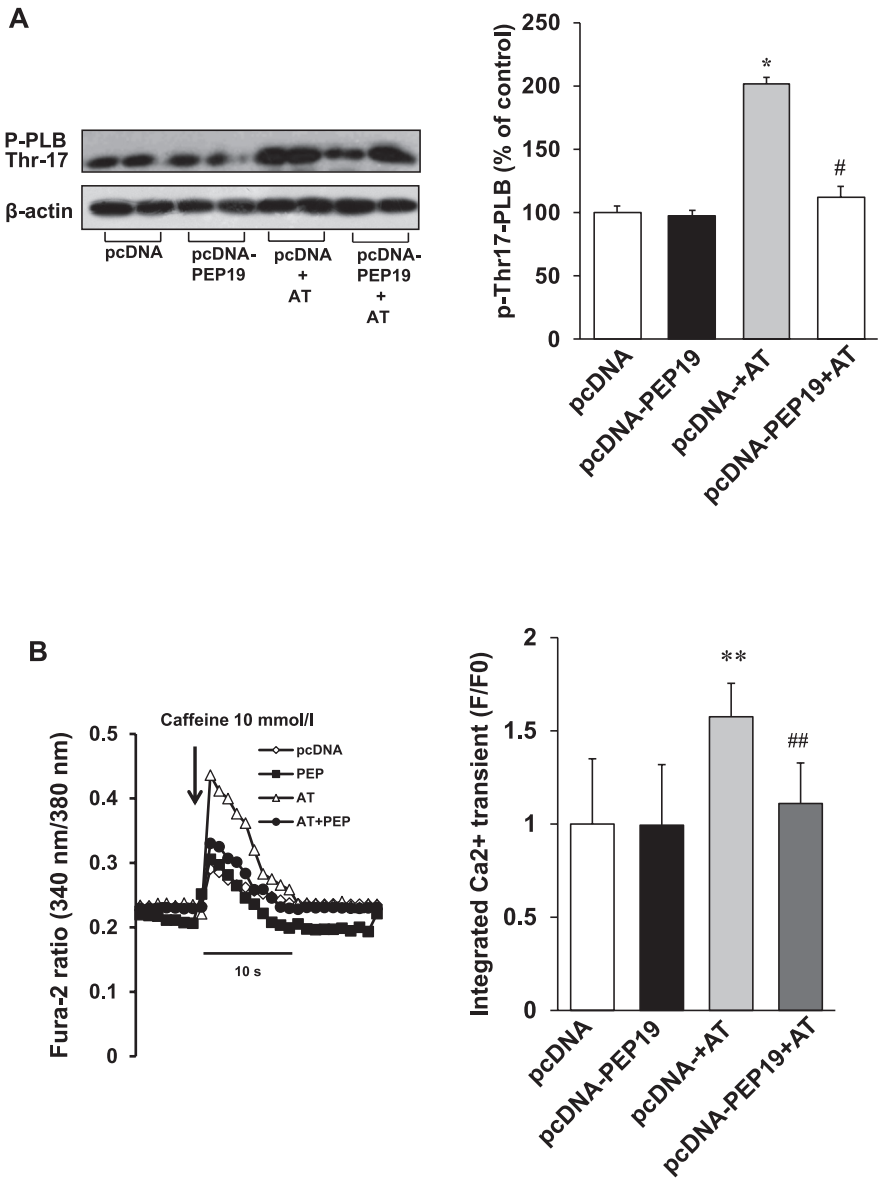

Fig. 5. Overexpression of PEP-19 decreased angiotensin II–induced phosphorylation of PLB and sarcoplasmic reticular Ca^{2+} concentration. The same samples described above were used for analysis of p-PLB and SR calcium. A) Phosphorylation of PLB at Thr-17 was examined. β-Actin was used as a loading control. Data are means ± S.E.M. of 3 independent experiments performed in triplicate. $^{*}P < 0.05$ vs. pcDNA, $^{\#}P < 0.05$ vs. pcDNA + AT. B) Caffine-induced Ca^{2+} release was performed using Fura-2. Fura-2 fluorescence intensity was monitored at 340/380 nm. Fluorescence intensity of pcDNA was arbitrarily defined as 1. Results are means ± S.E.M. of 3 independent experiments performed in triplicate. $^{**}P < 0.01$ vs. pcDNA, $^{\#\#}P < 0.01$ vs. pcDNA + AT.

intracellular signaling contributes to the pathological process of cardiac hypertrophy (3).

Although here we did not elucidate the precise mechanism of PEP-19 inhibition on the angiotensin II–mediated activities of CaMKII and CaN, we speculate that priority of PEP-19 binding to CaM might contribute to its inhibition on CaMKII and CaN. Autophosphorylation at Thr 287 in the autoinhibitory domain of CaMKIIδ occurs once the enzyme is activated by Ca^{2+}/Calmodulin binding and will generate autonomous activity of CaMKII (37 – 39). In addition, the dephosphorylation of NFATc3 as a CaN target protein was inhibited under PEP-19 transfection (40). We proposed that PEP-19 inhibits calmodulin activity and in turn suppresses the activation of Ca^{2+}/Calmodulin-dependent intracellular signaling, such as CaMKII and CaN, eventually inhibiting the pathological process of cardiomyocyte hypertrophy. This notion is supported by the observation that angiotensin II causes the disturbance of Cm (pF), Rin (MΩ), and RMP (resting membrane potential, mv) in cardiomyocytes, whereas this effect was partially alleviated by PEP-19 treatment. PLB phosphorylation also contributes to the increased contraction by elevating the concentration of stored Ca^{2+} in the sarcoplasmic reticulum. Consistent with the change in CaMKII autophosphorylation, treatment with 100 nM angiotensin II increased phospholamban Thr-17 phosphorylation at 48 h, indicating that increased PLB is likely to be a compensatory response to hypertrophic stimulation. By contrast, the increased phosphorylation of PLB caused

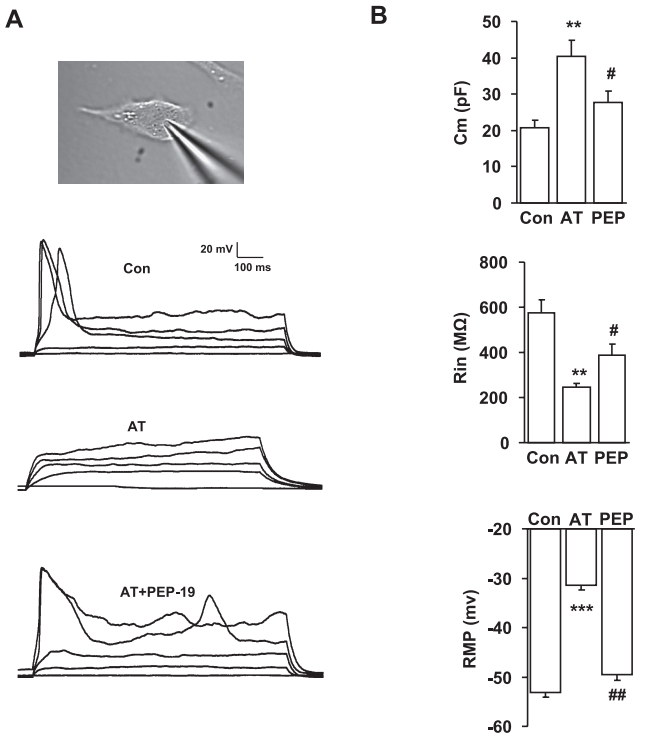

Fig. 6. Effect of PEP-19 transfection on the passive and active membrane properties of newborn culture cardiomyocytes in the presence of AT. A) Morphology of cardiomyocytes under an upright microscope (Olympus) equipped with a 40 × water-immersion lens (upper panel). Measure of action potential from control, AT stimulation and PEP-19 transfection group (lower panel), action potentials evoked with current injection (from bottom to top, −10 pA, −5 pA, 0 pA, 5 pA, and 10 pA). B) Effect of PEP-19 transfection on passive membrane properties of newborn culture cardiomycytes. Cm, membrane capacitance; R_{in}, membrane input resistance. Results are means ± S.E.M. of 3 independent experiments performed in triplicate. $^{**}P < 0.01$, $^{***}P < 0.001$ vs. pcDNA; $^{\#}P < 0.05$, $^{\#\#}P < 0.01$ vs pcDNA + AT.

by angiotensin II was blocked by PEP-19 overexpression. Nevertheless, there remains unresolved questions regarding the pathophysiological mechanisms of angiotensin II–mediated cardiovascular diseases. The cardiac angiotensin II type 1 receptor (AT1R) also plays a critical role in the molecular mechanism of cardiovascular hypertrophy, via activation of not only PLC but also a variety of intracellular signal transduction cascades (41, 42).

In conclusion, we suggested that the endogenous PEP-19 protein was inducible in heart suffering from hypertrophic stimulation. Upregulation of PEP-19 might be involved in an endogenous compensatory mechanism in the cardiomyocytes or heart to act against cardiac hypertrophy and failure. PEP-19 inhibits angiotensin II–induced cardiac hypertrophy through inhibition of integrated Ca^{2+} transient and in turn activation of CaMKII and CaN signaling. The further understanding of the function of PEP-19 during the pathological process of cardiac hypertrophy could have broad significance in the treatment of heart diseases.

Acknowledgments

This work was supported in part by Hangzhou City New Century 131 Excellent Youth Talent Project and Medical scientific research projects of Hangzhou (20130633B32).

References

1 Careno JE, Apablaza F, Ocaranza MP, Jalil JE. Cardiac hypertrophy: molecular and cellular events. Rev Esp Cardiol. 2006; 59:473–486.
2 Berridge MJ. Remodelling Ca^{2+} signalling systems and cardiac hypertrophy. Biochem Soc Trans. 2006;34:228–231.
3 Lu YM, Shioda N, Han F, Moriguchi S, Kasahara J, Shirasaki Y, et al. Imbalance between CaM kinase II and calcineurin activities impairs caffeine-induced calcium release in cardiomyocytes. Biochem Pharmacol. 2007;74:1727–1737.
4 Gruver CL, DeMayo F, Goldstein MA, Means AR. Targeted developmental overexpression of calmodulin induce proliferative and hypertrophic growth of cardiomyocytes in transgenic mice. Endocrinology. 1993;133:376–388.
5 Molkentin JD. Dichotomy of Ca^{2+} in the heart: contraction versus intracellular signaling. J Clin Invest. 2006;116:623–626.
6 Crabtree GR. Generic signals and specific outcomes: signaling through Ca^{2+}, calcineurin and NF-AT. Cell. 1999;96:611–614.
7 Klee CB, Ren H, Wang X. Regulation of the calmodulin stimulated protein phosphatase, calcineurin. J Biol Chem. 1998; 273:13367–13370.
8 Molkentin JD. Calcineurin-NFAT signaling regulates the cardiac hypertrophic response in coordination with the MAPK. Cardiovascular Research. 2004;63:467–475.
9 Molkentin JD, Dorn GW. Cytoplasmic signaling pathways that regulate cardiac hypertrophy. Annu Rev Physiol. 2001;63:391–426.
10 Hunter JJ, Chien KP. Signaling pathway for cardiac hypertrophy and failure. N Eng J Med. 1999;341:1276–1283.
11 Sangameswaran L, Hempstead J, Morgan JI. Molecular cloning of a neuron-specific transcript and its regulation during normal and aberrant cerebellar development. Proc Natl Acad Sci U S A. 1989;86:5651–5655.
12 Berrebi AS, Spirou GA. PEP-19 immunoreactivity in the cochlear nucleus and superior olive of the cat. Neuroscience. 1998;83:535–554.
13 Ziai MR, Pan Y-CE, Hulmes JD, Sangameswaran L, Morgan JI. Isolation, sequence and developmental profile of a brain specific polypeptide, PEP-19. Proc Natl Acad Sci U S A. 1986;83: 8420–8423.
14 Kanamori T, Takakura K, Mandai M, Kariya M, Fukuhara K, Kusakari T, et al. PEP-19 overexpression in human uterine leiomyoma. Mol Hum Report. 2003;9:709–717.
15 Slemmon JR, Martzen MR. Neuromodulin (GAP-43) can regulate a calmodulin-dependent target in vitro. Biochemistry. 1994;33:5653–5660.
16 Gerendasy DD, Herron SR, Watson JB, Sutcliffe JG. Mutational

and biophysical studies suggest RC3/neurogranin regulates calmodulin availability. J Biol Chem. 1994;269:22420–22426.
17 West MJ, Coleman PD, Flood DG, Troncoso JC. Difference in the pattern of hippocampal neuronal loss in normal ageing and Alzheimer s disease. Lancet. 1994;344:769–772.
18 Slemmon JR, Feng B, Erhardt JA. Small proteins that modulate calmodulin-dependent signal transduction: effects of PEP-19, neuromodulin and neurogranin on enzyme activation and cellular homeostasis. Mol Neurobiol. 2000;22:99–113.
19 Erhardt JA, Legos JJ, Johanson RA, Slemmon JR, Wang X. Expression of PEP-19 inhibits apoptosis in PC12 cells. Neuroreport. 2000;11:3719–3723.
20 Kanazawa Y, Makino M, Morishima Y, Yamada K, Nabeshima T, Shirasaki Y. Degradation of PEP-19, a calmodulin-binding protein, by calpain is implicated in neuronal cell death induced by intracellular Ca^{2+} overload. Neuroscience. 2008;154:473–481.
21 Jouannot P, Hatt P. Rat myocardial mechanics during pressure-induced hypertrophy development and reversal. Am J Physiol. 1975;229:355–364.
22 Laemmli UK. Cleavage of structure proteins during the assembly of the head of bacteriophage T4. Nature. 1970;227:680–685.
23 Fukunaga K, Yamamoto H, Matsui K, Higashi K, Miyamoto E. Purification and characterization of a Ca^{2+} and calmodulin-dependent protein kinase from rat brain. J Neurochem. 1982; 39:1607–1617.
24 Fukunaga K, Horikawa K, Shibata S, Takeuchi Y, Miyamoto E. Ca^{2+}/calmodulin-dependent protein kinase II-dependent long-term potentiation in the rat suprachiasmatic nucleus and its inhibition by melatonin. J Neurosci. 2002;70:799–807.
25 Fukunaga K, Muller D, Ohmitsu M, Bako E, DePaoli-Roach AA, Miyamoto E. Decrease protein phosphatase 2A activity in hippocampal long-term potentiation. J Neurochem. 2000;74: 807–811.
26 Lu YM, Shioda N, Yamamoto Y, Han F, Fukunaga K. Transcriptional upregulation of calcineurin Abeta by endothelin-1 is partially mediated by calcium/calmodulin-dependent protein kinase IIdelta3 in rat cardiomyocytes. Biochem Biophys Acta. 2010;1799:429–441.
27 Ku HC, Su MJ. DPP4 deficiency preserved cardiac function in abdominal aortic banding rats. PLoS One. 2014;9:e85634.
28 Manderfield VV, Patel GI, Fishman, Jonathan A. Myocardial notch signaling reprograms cardiomyocytes to a conduction-like phenotype. Circulation. 2012;126:1058–1066.
29 Utal AK, Stopka AL, Roy M, Coleman PD. PEP-19 immunohistochemistry defines the basal ganglia and associated structures in the adult human brain, and is dramatically reduced in Huntington's disease. Neuroscience. 1998;86:1055–1063.
30 Gerendasy DD, Sutcliffe JG. RC3/neurogranin, a postsynaptic calpacitin for setting the response threshold to calcium influxes. Mol Neurobiol. 1997;15:131–163.
31 Putkey JA, Kleerekoper Q, Gaertner TR, Waxham MN. 2003. A new role for IQ motif proteins in regulating calmodulin function. J Biol Chem. 2003;278:49667–49670.
32 Slemmon JR, Morgan JI, Fullerton SM, Danho W, Hilbush BS, Wengenack TM. Calmodulinstatins are peptide antagonists of calmodulin based upon a conserved structural motif in PEP-19, neurogranin, and neuromodulin. J Biol Chem. 1996;271:15911–15917.
33 Rudolph MC, McManaman JL, Phang T, Russell T, Kominsky DJ, Serkova NJ, et al. Metabolic regulation in the lactating mammary gland: a lipid synthesizing machine. Physiol Genomics. 2007;28:323–336.
34 Xiao J, Wu Y, Chen R, Lin Y, Wu L, Tian W, et al. Expression of Pcp4 gene during osteogenic differentiation of bone marrow mesenchymal stem cells in vitro. Mol Cell Biochem. 2008; 309:143–150.
35 Lu YM, Han F, Shioda N, Moriguchi S, Shirasaki Y, Qin ZH, et al. Phenylephrine-induced cardiomyocyte injury is triggered by superoxide generation through uncoupled endothelial nitric-oxide synthase and ameliorated by3-[2-[4-(3-chloro-2-methylphenyl)-1-piperazinyl]ethyl]-5,6-dimethoxyindazole (DY-9836), a novel calmodulin antagonist. Mol Pharmacol. 2009;75:101–112.
36 Lu YM, Shioda N, Han F, Kamata A, Shirasaki Y, Qin ZH, et al. DY-9760e inhibits endothelin-1-induced cardiomyocyte hypertrophy through inhibition of CaMKII and ERK activities. Cardiovasc Ther. 2009;27:17–27.
37 Zhang T, Brown JH. Role of Ca^{2+}/calmodulin-dependent protein kinase II in cardiac hypertrophy and heart failure. Cardiovasc Res. 2004;63:476–486.
38 Meyer T, Hanson PI, Stryer L, Schulman H. Calmodulin trapping by calcium-calmodulin-dependent protein kinase. Science. 1992; 256:1199–1202.
39 Johanson RA, Sarau HM, Foley JJ, Slemmon JR. Calmodulin-binding peptide PEP-19 modulates activation of calmodulin kinase II In situ. J Neurosci. 2000;20:2860–2866.
40 Selvetella G, Hirsch E, Notte A, Tarone G, Lembo G. Adaptive and maladaptive hypertrophic pathways: points of convergence and divergence. Cardiovasc Res. 2004;63:373–380.
41 Li Y, Kishimoto I, Saito Y, Harada M, Kuwahara K, Izumi T, et al. Guanylyl cyclase-A inhibits angiotensin II type 1A receptor-mediated cardiac remodeling, an endogenous protective mechanism in the heart. Circulation. 2002;106:1722–1728.
42 Zhai P, Yamamoto M, Galeotti J, Liu J, Masurekar M, Thaisz J, et al. Cardiac-specific overexpression of AT1 receptor mutant lacking Galpha q/G alpha i coupling causes hypertrophy and bradycardia in transgenic mice. J Clin Invest. 2005;115: 3045–3056.